

**Evidence for a SN₂-Type Pathway in the Exchange of
Phosphines at a [PhSe]⁺ Centre**

Journal:	<i>Dalton Transactions</i>
Manuscript ID:	DT-ART-07-2014-002253.R1
Article Type:	Paper
Date Submitted by the Author:	15-Sep-2014
Complete List of Authors:	Russell, Christopher; University of Bristol, Inorganic and Materials Chemistry Section Forfar, Laura; University of Bristol, chemistry Green, Michael; University of Bristol, School of Chemistry Haddow, Mairi; University of Bristol, Hussein, Sharifa; University of York, chemistry Lynam, Jason; University of York, chemistry Slattery, John; University of York, Department of Chemistry

ARTICLE

Evidence for a S_N2-Type Pathway in the Exchange of Phosphines at a [PhSe]⁺ Centre

Cite this: DOI: 10.1039/x0xx00000x

Laura C. Forfar,^a Michael Green,^a Mairi F. Haddow,^a Sharifa Hussein,^b Jason M. Lynam,^b John M. Slattery^b and Christopher A. Russell^a

Received 00th January 2012,
Accepted 00th January 2012

DOI: 10.1039/x0xx00000x

www.rsc.org/

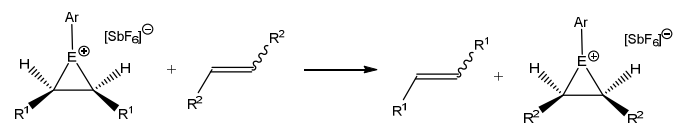
A range of thio- and seleno-phosphonium cationic complexes [RE(PR'₃)⁺][X]⁻ (R = Me, Ph; E = S, Se; X = GaCl₄, SbF₆) have been synthesised and structurally characterised. Reaction of [PhSPPPh₃][GaCl₄] and [PhSePPh₃][GaCl₄] with P^tBu₃ results in the ready transfer of the “RS⁺” and “RSe⁺” fragments from PPh₃ to the stronger electron donor P^tBu₃. NMR experiments combined with an Eyring analysis on the corresponding degenerate phosphine exchange reaction allowed the thermodynamic values for the phosphine exchange reaction of the sulfur cation (ΔH^\ddagger 18.7 ± 12.0 kJ mol⁻¹; ΔS^\ddagger -99.3 ± 36.3 J mol⁻¹ K⁻¹) to be compared with the corresponding values (ΔH^\ddagger 2.4 ± 1.1 kJ mol⁻¹ and ΔS^\ddagger -58.1 ± 5.0 J mol⁻¹ K⁻¹) for the [PhSePPh₃]⁺ system. Importantly, the large negative entropy of activation and linear dependence on the rate of exchange are compatible with an S_N2-type exchange process. This conclusion is supported by DFT calculations which confirm that the phosphine exchange process occurs via an associative mechanism. The rate of exchange was found to increase from sulfur to selenium and those with aryl substituents underwent exchange faster than those with alkyl substituents.

Introduction

Sulfur- and selenium-based reagents have become an essential part of the armoury of synthetic organic chemists with important applications in pharmaceuticals,¹ biochemistry² and ligand chemistry.³ This can be related to the fact that the introduction of organo-heteroatom moieties C–E (E = S, Se) leads to activated polar bonds due to electronegativity differences between carbon and the heteroatom and the presence of unshared electron pairs with the consequence that the C–E bonds stabilise α-carbocations, α-carbanions, carboradicals and β-carbocations.⁴ In addition, and of particular relevance to this current contribution, inorganic chemists have sought a greater insight into the structure, bonding and reactivity of cationic chalcogen centres, in particular of Se and Te.⁵

Recently,⁶ attention has focused on the reactivity of thiiranium and seleniranium cations and the possibility of observing direct [ArE]⁺ transfer to alkenes as is illustrated in Scheme 1. Two limiting mechanisms can be envisioned for such a transfer process, in which the [ArE]⁺ cation departs unassisted and is then captured by another alkene (*i.e.*, a dissociative process), or another alkene assists in the process (*i.e.*, an associative process). However, it has been calculated⁷ that the enthalpic barrier (134 kJ mol⁻¹) for the direct dissociation of an uncoordinated [ArE]⁺ is prohibitively high at room temperature in the gas phase, moreover, computational studies by Radom and coworkers⁸ on the direct transfer of a [ArE]⁺ cation between two alkenes also suggest both a

relatively low kinetic barrier (~46 kJ mol⁻¹) and a relationship to an analogous S_N2 type exchange process with phosphonium systems⁹ (Scheme 2).



Scheme 1 Transfer of [ArE]⁺ between alkenes

Furthermore, Borodkin¹⁰ computationally evaluated the enthalpic barrier for direct, intramolecular, thiiranium-alkene and seleniranium-alkene transfer, and found that the barrier to transfer is in the order [RS]⁺ > [ArS]⁺ > [RSe]⁺.



Scheme 2 S_N2 type exchange process with alkenes at [ER]⁺ and comparison with the corresponding phosphonium systems

Importantly, Denmark and co-workers have recently^{6b} found experimental evidence to support this order of reactivity in an apparent associative process and have also suggested¹¹ a related S_N2 type transition state (Figure 1) for catalytic, asymmetric seleno-etherification reactions.

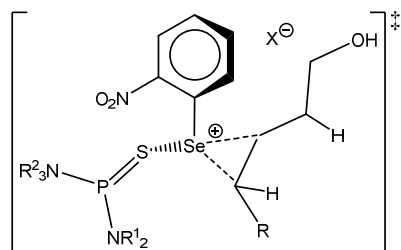


Figure 1 Proposed transition state for asymmetric seleno-etherification reactions

Results and discussion

Although these new insights into the mechanisms of such exchange processes are important, to our knowledge these proposals have not been reinforced by experimental data, even at the relatively simple level of providing proof that an associative pathway is preferred to a dissociative process. As detailed in our recent paper¹² we have successfully studied exchange processes at a phosphonium centre using NMR techniques and this has encouraged us to use related methods to establish the likely mechanism by which exchange reactions occur at a $[RSe]^+$ centre.

As a first step we sought to probe the exchange of alkenes at the cationic RE^+ centre. Latent sources of PhE^+ were generated from the mixture of $PhECl$ ($E = S, Se$) with a halide abstractor (gallium trichloride or silver hexafluoroantimonate) in dichloromethane.¹³ The subsequent reaction (for $E = Se$) with a stoichiometric amount of norbornene was followed by 1H NMR spectroscopy, which showed the diagnostic alkene peaks of the norbornene moved upfield (to $\delta = 5.95$ ppm; *cf.* 6.01 ppm for free norbornene under the same conditions). This is consistent with binding to the RSe^+ centre and subsequent addition of an excess of norbornene revealed only one olefinic peak in the 1H NMR spectrum which is suggestive of rapid alkene exchange on the NMR timescale. However, poor solubility at moderate- and low-temperatures meant this system was not conducive to detailed kinetic analysis and thus attention moved from alkenes to the related phosphine complexes, which could be followed unambiguously by ^{31}P NMR spectroscopy.

These were readily prepared using the protocol for the generation of $[RE]^+$ sources described above, followed by addition of triphenylphosphine. This resulted in the formation of ionic quasi-phosphonium salts $[PhSPPPh_3][X]$ (**1**) and $[PhSePPh_3][X]$ (**2**) ($X = GaCl_4, SbF_6$).[†] Crystals suitable for single-crystal X-ray diffraction were grown from dichloromethane solutions layered with *n*-hexane.

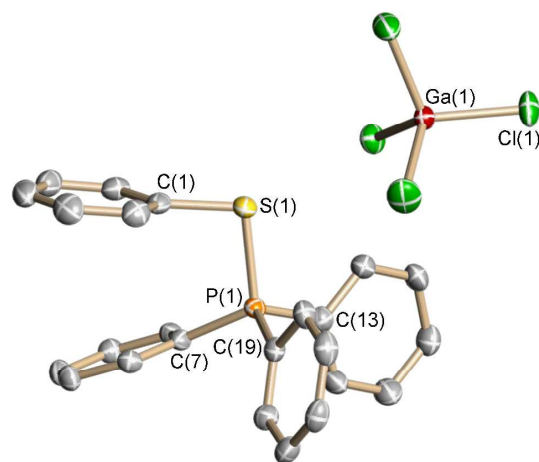


Figure 1 – Molecular structure of **1**. Hydrogen atoms have been omitted for clarity. Selected bond lengths (Å) and angles (°): P(1)-S(1) 2.0774(5), C(1)-S(1) 1.7887(16), C(1)-S(1)-P(1) 99.61(5), C(7)-P(1)-S(1) 108.81(5), C(13)-P(1)-S(1) 106.43(5), C(19)-P(1)-S(1) 111.64(5), C(7)-P(1)-C(13) 110.74(7), C(7)-P(1)-C(19) 110.76(7), C(19)-P(1)-C(13) 108.40(6).

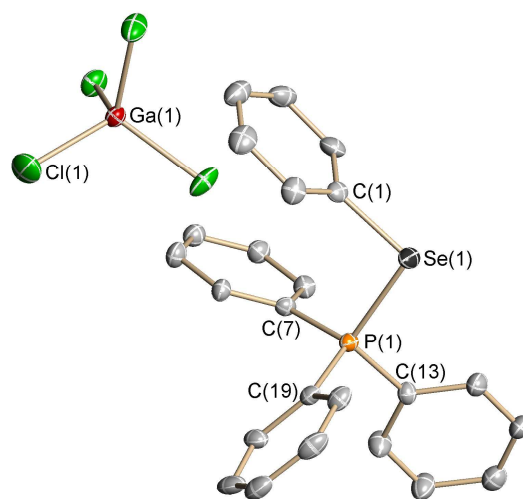


Figure 2 – Molecular structure of **2**. Hydrogen atoms have been omitted for clarity. Selected bond lengths (Å) and angles (°): P(1)-Se(1) 2.2318(9), C(1)-Se(1) 1.917(3), C(1)-Se(1)-P(1) 96.71(10), C(7)-P(1)-Se(1) 108.57(10), C(13)-P(1)-Se(1) 112.00(11), C(19)-P(1)-Se(1) 107.18(11), C(7)-P(1)-C(13) 110.41(15), C(7)-P(1)-C(19) 110.46(15), C(13)-P(1)-C(19) 108.18(15).

The solid-state structures (Figures 1 and 2) shows the PhE unit bonded to PPh_3 forming a formal phosphonium cation with a tetrachlorogallate anion. Both structures are essentially ion-separated, with the closest distance between E and the closest approaching chloride of the $[GaCl_4]^-$ anions ($E = S, Se$; $X = Cl$) in **1** (3.639 Å) and **2** (3.633 Å) being close to the sum of the Van der Waals radii (3.55 Å, 3.65 Å). Within the cationic moieties, the acute C-E-P bond angles of 99.61(5)° ($E = S$) and 96.71(10)° ($E = Se$) arise from the presence of π -stacking effects of the phenyl rings. The angle between the planes of the phenyl rings for the selenium structure was 22.91° and for the sulfur analogue 24.77° with the tighter angle for the selenium

complex arising from the larger size of selenium. The closest inter-ring distance ($C_{\text{ipso}}-C_{\text{ipso}}$) is 3.177 Å for Se and 3.105 Å for S, highlighting the close proximity of the rings as a result of this $\pi-\pi$ interaction. As expected the S-P bond length of 2.0774(5) Å is smaller than the Se-P bond distance of 2.2318(9) Å.

The ^{31}P NMR spectrum of **2** shows a sharp singlet at 38.3 ppm with characteristic selenium satellites (^{77}Se , 7.63%, $I = \frac{1}{2}$) and compound **1** gives a ^{31}P NMR resonance at 46.7 ppm.

Reaction of **1** and **2** with more strongly donating phosphines resulted in the displacement of triphenylphosphine and transfer of the EPh^+ unit to the more basic phosphine. This reaction could be followed *in situ* with the ^{31}P NMR spectrum of the reaction mixture showing a peak for the product $[\text{PhSP}^{\text{E}}\text{Bu}_3][\text{X}]$ (**3**) at 85.7 ppm and $[\text{PhSeP}^{\text{E}}\text{Bu}_3][\text{X}]$ (**4**) 89.0 ppm and a peak for free PPh_3 at *ca.* -5 ppm. Layering of the reaction mixture with *n*-hexanes resulted in a crop of crystals suitable for single crystal X-ray diffraction and the solid-state structures are shown in Figures 3 and 4 respectively.

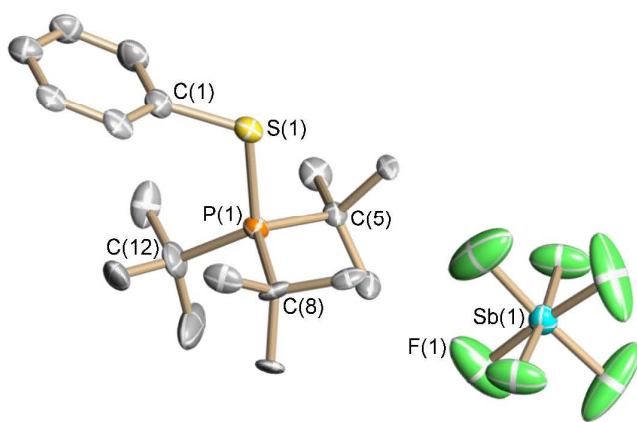


Figure 3 - Molecular structure of **3**. Hydrogen atoms have been omitted for clarity. Selected bond lengths (Å) and angles ($^\circ$): P(1)-S(1) 2.096(7), S(1)-C(1) 1.826(12), C(1)-S(1)-P(1) 112.6(5), C(7)-P(1)-S(1) 115.2(6).

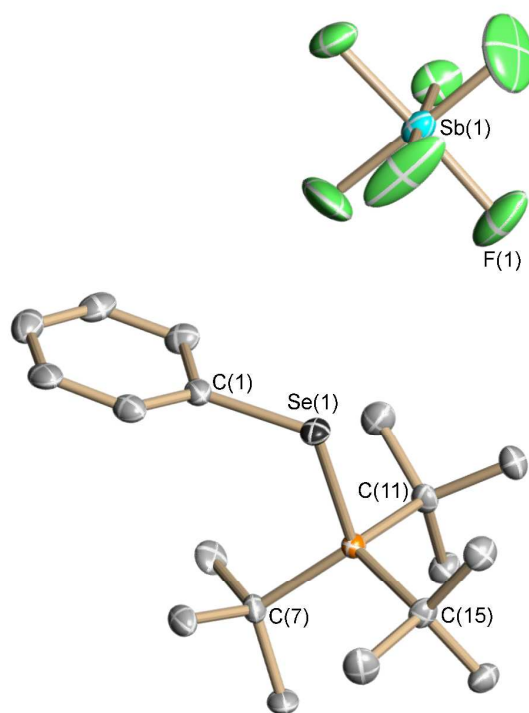


Figure 4 – Molecular structure of **4**. Hydrogen atoms have been omitted for clarity. Selected bond lengths (Å) and angles ($^\circ$): C(1)-Se(1) 1.930(3), Se(1)-P(1) 2.2528(8), C(1)-Se(1)-P(1) 107.99(10), C(7)-P(1)-Se(1) 113.48(10).

Compound **3** displays pronounced site disorder in both the SPh fragment and in the ^tBu groups, resulting in a low quality final data set. However, despite this it is clear from both the solid-state structures and the solution data show the EPh^+ fragment has been transferred onto the stronger donor phosphine forming new phosphonium cations. There are subtle geometrical differences in the structure of **1** and **2** (PPh_3) and **3** and **4** ($^t\text{PBu}_3$). The C-E-P angles have opened up to 112.6(5) $^\circ$ (E = S) and 107.99(10) $^\circ$ (E = Se) potentially due to the elimination of π -stacking effects and/or the steric repulsion between ^tBu groups and the E-Ph group. The E- $^t\text{PBu}_3$ bond lengths are slightly longer than the E- PPh_3 bond distances at 2.096(7) Å (E = S) and 2.253(1) Å (E = Se) which is the opposite of what was expected for a more donating phosphine (see the DFT discussion below for an explanation of this apparent anomaly).

The transfer of the cationic Eph fragment to different phosphines was monitored by ^{31}P NMR spectroscopy and substitution occurs with a number of more strongly donating phosphines including, but not limited to, trimethylphosphine and tricyclohexylphosphine. No exchange was witnessed when using large, relatively weakly donating phosphines (for example tri(*o*-tolyl)phosphine).

Seleno- and thio-phosphonium salts have been previously reported in the literature. Tetramers of the type $\text{Ph}_4\text{Se}_4\text{Br}_4$ and $(\text{Ph}_2\text{Se}_2\text{I}_2)_2$, formed from the reaction of Ph_2Se_2 and Br_2 ¹⁴ and Ph_2Se_2 and I_2 ,¹⁵ were reacted with 4 equivalents of PR_3 .¹⁶ Following the observation that the basicity of the phosphine directs the structural connectivity of the product, a range of phosphines were studied and the products analysed both in the solid state and in solution. Highly basic phosphines resulted in a lengthening of the E-P bond which in extreme cases yielded an ion separated product. These structures are fluxional in

solution, forming $[\text{Ph}_3\text{PI}][\text{SePh}]$ as shown by broader signals in the ^{31}P NMR spectrum and loss of P-Se coupling. It was observed that a slight excess of phosphine in the ^{31}P NMR spectrum showed time averaged signals however no further experiments investigating this exchange have been reported.¹⁷

An excess of triphenylphosphine was added to the reaction mixtures resulting in the observation of additional peaks in the ^{31}P NMR spectrum.¹² Upon further investigation it was found that free PPh_3 was exchanging with the coordinated PPh_3 and that the rate of this exchange varied with the specific organochalcogen moiety being studied. Thus these systems seemed an ideal vehicle to gain insight into these degenerate exchange processes at chalcogen centres. Hence the exchange mechanisms were probed by NMR titrations combined with variable temperature and exchange spectroscopy experiments and finally line shape analysis. This allowed for thermodynamic values to be extracted from an Eyring analysis of the exchange-rate data.

Sequential addition of stoichiometric equivalents of PPh_3 to $[\text{PhSPPH}_3]^+[\text{GaCl}_4]^-$ revealed a slow exchange on the NMR timescale with resonances associated with both coordinated and uncoordinated phosphine species. Upon heating the sample to 100°C the peaks did not coalesce but exchange was confirmed by a ^{31}P EXSY experiment. In contrast, addition of 1 equivalent of PPh_3 to $[\text{PhSePPH}_3]^+[\text{GaCl}_4]^-$ led to the disappearance of the peak for the complex at 38.3 ppm, and the emergence of a resonance at 16.4 ppm with the loss of selenium satellites, a phenomenon typically associated with rapid bond cleavage on the NMR timescale. Addition of further equivalents of PPh_3 led to a gradual upfield shift of the signal towards that of free PPh_3 , for example, reaction of **1** with 4 equivalents of PPh_3 gave a

single peak in the ^{31}P NMR spectrum at 2.9 ppm. These data indicated that in the case of $[\text{PhSePPH}_3]^+$ exchange between free and coordinated phosphine was occurring more rapidly on the NMR timescale compared to the sulfur system. At low temperatures (-90°C) the peaks did not decoalesce, showing that fast exchange was still occurring under these conditions.

The exchange process for both the sulfur- and selenium-substituted systems was modelled by line shape analysis using the gNMR program. The resulting data demonstrated that the rate of exchange increased in an approximate linear fashion with increasing concentration of added phosphine. By determining the rate constants for exchange over a range of temperatures it was possible to extrapolate activation parameters using the Eyring equation. In the case of the sulfur-substituted system the calculated parameters were ΔH^\ddagger (18.7 ± 12.0) kJ mol^{-1} and ΔS^\ddagger (-93.6 ± 36.3) $\text{J mol}^{-1} \text{K}^{-1}$, whereas for $[\text{PhSePPH}_3]^+$ the barriers for exchange were ΔH^\ddagger (2.4 ± 1.1) kJ mol^{-1} and ΔS^\ddagger (-52.4 ± 5.0) $\text{J mol}^{-1} \text{K}^{-1}$. The large, negative entropy of activation and approximate linear dependence of rate of exchange with phosphine concentration are consistent with a second order S_N2 -type process. It also appears that the slower rate of exchange at sulfur has both an entropic and enthalpic contribution.

DFT studies

In order to gain additional understanding of the systems described here we undertook a computational study to explore the structure and bonding in phosphine complexes of $[\text{EPh}]^+$ ($\text{E} = \text{S}, \text{Se}$) and the mechanistic features of phosphine ligand

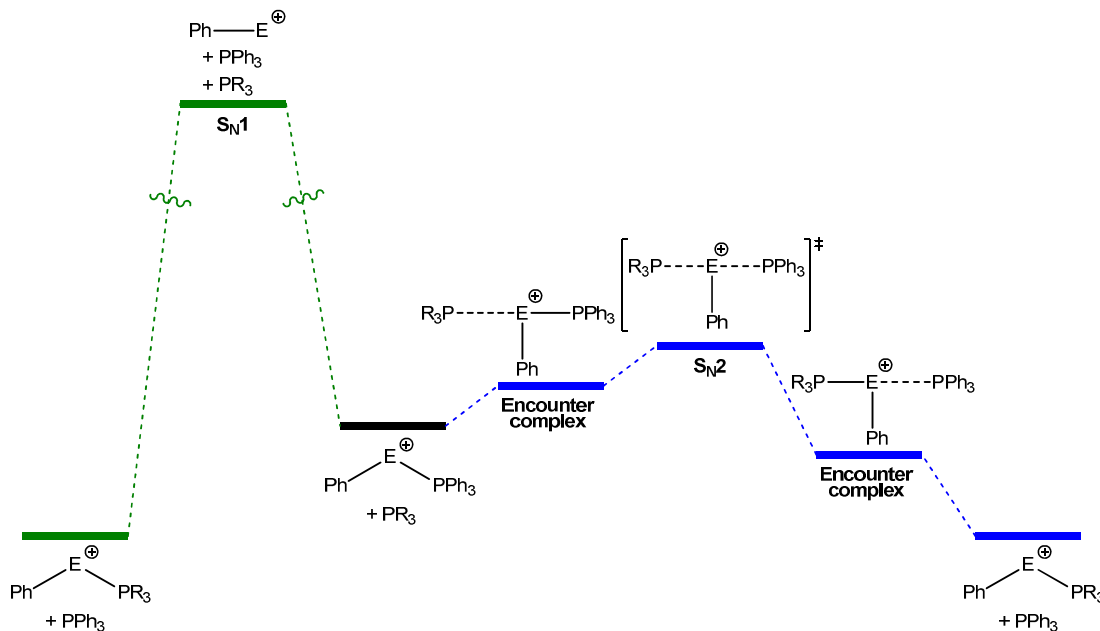


Figure 5 – Two mechanistic pathways for phosphine exchange at $[\text{EPh}]^+$ ($\text{E} = \text{S}, \text{Se}$). On the left hand side a dissociative S_N1 -like mechanism and on the right hand side an associative S_N2 -like mechanism, which proceeds *via* the formation of an encounter complex prior to the transition state.

exchange at these cations. Full details of the computational studies are given in the ESI.

One unusual feature observed in the solid-state structures of the phosphine above is that the E-P bond lengths (for both $\text{E} = \text{S}$ and Se) increase when PPh_3 is substituted for P^tBu_3 . On the basis of donor strength, with P^tBu_3 being the better donor, one would expect the opposite effect. One possible explanation for

this is that π - π stacking present in the $[\text{PhE}(\text{PPh}_3)]^+$ salts brings the phosphine closer to the $[\text{PhE}]^+$ fragment in these ions. However, as in the solid-state structures, the E-P distances in the DFT optimised structures are shorter for the PPh_3 complexes than for the P^tBu_3 complexes at all levels of theory ((RI-)BP86/SV(P), (RI-)BP86/def2-TZVPP, (RI-)BP86-D3/SV(P) and (RI-)BP86-D3/def2-TZVPP levels, see ESI for

details), even when a functional is used that does not model π - π interactions that well. This suggests that this structural difference is not due to the π - π interactions in the PPh_3 complexes. In order to probe the bonding in these species in more detail we undertook an NBO analysis on the $[\text{PhE}(\text{PR}_3)]^+$ ($\text{E} = \text{S}, \text{Se}$; $\text{R} = \text{Ph}, \text{tBu}$) ions (at the BP86/SVP level). The Wiberg bond indices for the E-P bonds increase slightly on moving from PPh_3 to P^tBu_3 (from 0.966 to 1.006 for S and from 0.953 to 0.987 for Se). There is also some evidence of more significant hyperconjugation from the E-lone pairs to the P-C σ^* orbitals for the P^tBu_3 complexes compared to the PPh_3 complexes (e.g. average P-C σ^* occupation for the PPh_3 complexes = 0.084 and 0.082 e^- for S and Se respectively; for the P^tBu_3 complexes = 0.108 and 0.104 e^- for S and Se respectively). These features suggest stronger E-P bonding in the P^tBu_3 complexes, which is consistent with the experimental observations that PPh_3 is preferentially exchanged for P^tBu_3 at these cations. As such, it seems likely that the longer P-C bonds for the P^tBu_3 complexes compared to the PPh_3 complexes may simply be a steric effect due to the larger P^tBu_3 ligand.

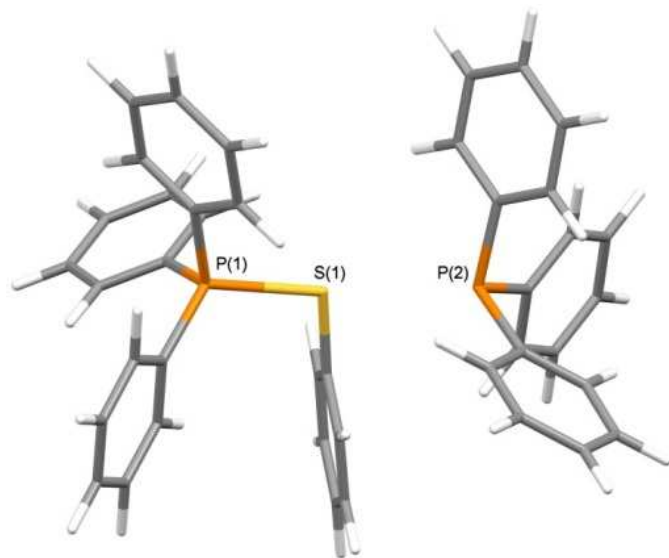


Figure 6 – Optimised structure of the encounter complex $[\text{PhSPPh}_3.\text{PPh}_3]^+$ at the BP86/SV(P) level. Selected bond lengths (Å): P(1)-S(1) 2.228, P(2)-S(1) 2.948.

Two potential phosphine exchange mechanisms were probed in the computational studies. A dissociative mechanism involving phosphine loss to give the intermediate $[\text{PhE}]^+$ and an associative mechanism proceeding through the transition state $[(\text{Ph}_3\text{P})\cdots\text{E}(\text{Ph})\cdots(\text{PPh}_3)]^+$ (Figure 5). As has been seen previously for phosphine-exchange reactions in $[\text{R}_4\text{C}_4\text{P}(\text{PR}_3)]^+$ ions,¹² the associative mechanism begins with the formation of an “encounter complex”, where the incoming phosphine ligand forms a weak interaction with the $[\text{PhE}(\text{PPh}_3)]^+$ ion (Figure 6). This is followed by the ligand-exchange transition state and formation of a new encounter complex where the free and coordinated phosphine ligands have been exchanged.

The NMR spectroscopic measurements described above allow for the performance of different levels of theory to be assessed against the experimental kinetic parameters (see ESI for full details). This showed that on balance, probably due to fortuitous error cancellation, the BP86/SV(P) level provides the best agreement between experiment and theory and this level

will be used in the discussion below. It is also clear that solvation effects, modelled here using the COSMO solvation model (with $\epsilon = 8.93$ for CH_2Cl_2 at 25 °C) are crucial to reproduce the experimental observations and values discussed below include these solvation corrections.

The computational study supports the experimental evidence that phosphine exchange for the $[\text{PhEPR}_3]^+$ ($\text{E} = \text{S}, \text{Se}$) cations occurs *via* an associative rather than a dissociative mechanism. Phosphine loss from $[\text{PhEPR}_3]^+$ is highly unfavourable for both sulfur and selenium, leading to ΔH^\ddagger of 295 and 280 kJ mol^{-1} respectively ($\Delta G^\ddagger = 247$ and 233 kJ mol^{-1}) (see Table 2).[‡] However, these data are slightly misleading, as the highly Lewis acidic $[\text{PhE}]^+$ ions that are formed are likely to be stabilised by, or react with, anions present in solution. Indeed, if a $[\text{GaCl}_4]^-$ ion is introduced to the $[\text{PhE}]^+$ ions in the computational study then geometry optimisations lead to formal halide abstraction from $[\text{GaCl}_4]^-$ to form the GaCl_3 adducts PhECl.GaCl_3 , which are significantly more stable (both in the gas phase and in CH_2Cl_2 solution) than $[\text{PhE}]^+$ and $[\text{GaCl}_4]^-$. This leads to lower, but still large, enthalpies of activation for the $\text{S}_{\text{N}}1$ -like mechanism (161 and 132 kJ mol^{-1} for S and Se respectively). Anion effects did not significantly change the relative energies for key states in the $\text{S}_{\text{N}}2$ -like mechanism (see ESI for details) and are not included here.

In contrast to the high barriers for the $\text{S}_{\text{N}}1$ -like mechanism, formation of the encounter complex is slightly endothermic for the reaction of $[\text{PhS}(\text{PPh}_3)]^+$ with PPh_3 or P^tBu_3 (+8 and +6 kJ mol^{-1} respectively) and slightly exothermic for the reaction of $[\text{PhSe}(\text{PPh}_3)]^+$ with PPh_3 or P^tBu_3 (-6 and -17 kJ mol^{-1} respectively). Subsequent formation of the associative ligand-exchange transition state leads to ΔH^\ddagger for the reaction of $[\text{PhS}(\text{PPh}_3)]^+$ with PPh_3 or P^tBu_3 of +15 and +4 kJ mol^{-1} respectively and for reaction of $[\text{PhSe}(\text{PPh}_3)]^+$ with PPh_3 or P^tBu_3 of -7 and -16 kJ mol^{-1} respectively. These data are consistent with the experimental observation of a small, positive ΔH^\ddagger for PPh_3 exchange at $[\text{PhS}(\text{PPh}_3)]^+$ and the smaller ΔH^\ddagger for P^tBu_3 exchange at this cation is consistent with the faster kinetics observed experimentally. Interestingly, the “transition states” for phosphine exchange at $[\text{PhSe}(\text{PPh}_3)]^+$ are not first-order saddle points on the potential energy surface, but rather are minima (representing a bis-phosphine complex of $[\text{PhSe}]^+$). The formation of these states from $[\text{PhSe}(\text{PPh}_3)]^+$ and PR_3 is actually slightly exothermic, although when entropy effects are taken into account the formation of these bis-phosphine complexes is endergonic, which is consistent with the experimental observation of mono phosphine complexes in solution and the solid state.

Table 2 – Summary of energetic data at the BP86/SV(P) level (including COSMO solvation in CH₂Cl₂ for all energies and anion effects ([GaCl₄]⁻) for the S_N1-like mechanism) for associative and dissociative phosphine exchange mechanisms.

	[PhS(PPh ₃)] ⁺	[PhSe(PPh ₃)] ⁺
$\Delta_{\text{rxn}}H$ (PPh ₃ encounter) (kJ mol ⁻¹)	8	-6
ΔH^\ddagger (PPh ₃ S _N 2) (kJ mol ⁻¹)	15	-7
ΔS^\ddagger (PPh ₃ S _N 2) (J K ⁻¹ mol ⁻¹)	-142	-123
ΔH^\ddagger (PPh ₃ S _N 1) (kJ mol ⁻¹)	161	132
$\Delta_{\text{rxn}}H$ (P ^t Bu ₃ encounter) (kJ mol ⁻¹)	6	-17
ΔH^\ddagger (P ^t Bu ₃ S _N 2) (kJ mol ⁻¹)	4	-16
ΔS^\ddagger (P ^t Bu ₃ S _N 2) (J K ⁻¹ mol ⁻¹)	-176	-121
ΔH^\ddagger (P ^t Bu ₃ S _N 1) (kJ mol ⁻¹)	161	132
$\Delta_{\text{rxn}}H$ (P ^t Bu ₃ exchange) (kJ mol ⁻¹)	-21	-25

The differences in energetics and reactivity seen between the S and Se systems suggests that the Se-cation [PhSe(PPh₃)]⁺ is significantly more Lewis acidic than its sulfur analogue. This may have its origins in the fact that Se is significantly larger, and thus there is less steric repulsion when forming the bis-phosphine complex for Se. However, electronic effects are also likely to be important. The Se centre in [PhSe(PPh₃)]⁺ carries a larger positive charge than the S in [PhS(PPh₃)]⁺ {0.086 vs. 0.014 (PABOON charges at the BP86/SV(P) level) or 0.201 vs. 0.039 (NBO charges at the BP86/SVP level)}. The LUMO of [PhSe(PPh₃)]⁺, (which is antibonding with respect to Se-P bonding, see Figure 7) is also lower in energy for the Se system compared to the S system (-5.923 vs. -5.835 eV). Both of these features are consistent with the more electrophilic behaviour of the Se cations and help to explain the differences in reactivity observed experimentally. Plots of the electrostatic potentials for these cations (figure 7) also show a difference in charge density, and distribution, between S and Se. A region of more positive electrostatic potential (the so-called “ σ -hole”) can clearly be seen at Se, but this is significantly less pronounced in the case of S. Since the σ -hole points directly towards any incoming nucleophile it is likely to be important in the formation of both the encounter complexes and S_N2-like transition states for phosphine exchange in these systems. A more prominent σ -hole in the case of Se is consistent with faster phosphine exchange kinetics and lower energy intermediates in the associative phosphine exchange mechanism compared to S.

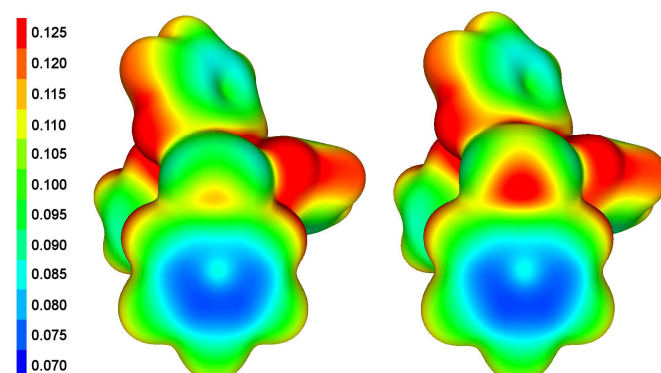
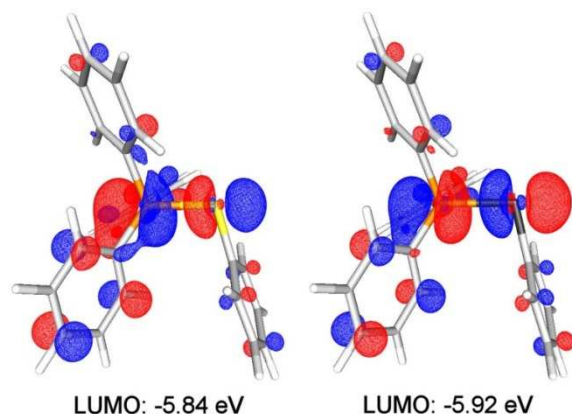


Figure 7 – (Above) LUMOs for the [PhE(PPh₃)]⁺ ions (E = S (left), Se (right) at the BP86/SV(P) level). (Below) The electrostatic potential (in a.u.), mapped on to the total electron density (isosurface at 0.002 a.u.), for the [PhE(PPh₃)]⁺ ions (E = S (left), Se (right) at the BP86/SV(P) level). S and Se are shown in the centre of the plots and the viewer is looking directly down the E-P bond in both cases.

Experimental studies with alkylchalcogeno phosphonium cations

Seleno-phosphonium salts with alkyl substituents at selenium have received less attention from the research community. Jones *et al.*, reported the solid-state structure of [Ph₃PSeMe][ClO₄], synthesised from reaction of (MeSe)₂ with Ph₃PAuCl and AgClO₄.¹⁸ Previous computations calculating the activation barriers for alkene transfer from thiiranium and seleniranium compounds predicted ‘iranium’ salts bearing an alkyl substituent had the highest barrier for transfer.¹⁹

[MeEPPH₃][SbF₆] (E = S (**5**), Se (**6**)) was prepared from the reaction of (MeE)₂ with silver hexafluoroantimonate in dichloromethane and the addition of one equivalent of triphenylphosphine. Characterisation was limited to that obtained from the NMR spectra of crude solutions which show a peak in the ³¹P NMR spectrum at 37.4 ppm with selenium satellites (*J*_{P-Se} 453 Hz) was supportive of the formation of the desired product, [MeSePPh₃][SbF₆]. Furthermore, addition of tri-*tert*-butylphosphine gave rise to a ³¹P NMR resonance at δ = 84.09 ppm with selenium satellites (¹*J*_{PSe} 458 Hz) accompanied by a signal at -4.6 ppm corresponding to uncoordinated triphenylphosphine, again supporting the production of [MeSeP^tBu₃][SbF₆].

Both **5** and **6** were amenable to kinetic studies of degenerate phosphine exchange. Thus, addition of one equivalent of triphenylphosphine to [MeSePPh₃][SbF₆] resulted in the observation of a solitary time-averaged signal upfield for that of free **6** in the ³¹P NMR spectrum, with the peak being broad at 14.3 ppm for reaction of **6** with 1 equivalent of PPh₃, and relatively sharp at -4.6 ppm for reaction with a 4-fold excess of PPh₃. Impurities in the starting material, which could not be removed by distillation, led to the formation of [Ph₃POH][SbF₆] (³¹P δ 21.5 ppm) and a peak at 36 ppm with selenium satellites of 734 Hz. Lineshape analysis of this data reveals that, in a similar vein to the phenyl-substituted analogue, that the rate of exchange showed a linear relationship to the concentration of added PPh₃.

Complex **5** was amenable to a similar study of reactivity and kinetics. Thus, the peak in the ³¹P NMR spectrum at 47.1 ppm was assigned to [MeSPPh₃][SbF₆], in comparison with the resonance for the similar compound [PhSPPh₃][SbF₆]. Furthermore, addition of tri-*tert*-butylphosphine gave rise to a signal at 82.0 ppm accompanied by another at -4.6 ppm, consistent with uncoordinated triphenylphosphine, again

showing exchange of the sulfuranyl cation to the more basic phosphine.

Once again the kinetics of phosphine exchange were examined by monitoring the reaction of **5** with additional PPh₃. However, in contrast to all other systems examined in this study, further triphenylphosphine did not exchange with the coordinated phosphine and the peak for the starting complex was retained along with appearance of a peak for free PPh₃. To test for a very slow exchange this reaction mixture was probed by ³¹P EXSY. A variety of mixing times were tested to find optimum conditions for exchange. However, no exchange was observed under these conditions and only the diagonal peaks conforming to the starting complex and free triphenylphosphine were detected.

Experimental

All reactions were performed under an atmosphere of nitrogen or argon using standard Schlenk line and glove box techniques; solvents were dried using an Anhydrous Engineering Grubbs-type system (alumina columns). PhSeCl, PhSSPh, MeSeSeMe, MeSSMe, GaCl₃, AgSbF₆, PPh₃ and P^tBu₃ were of analytical grade, obtained from commercial suppliers and used without further purification. PhSCl was prepared by literature procedures.²⁰ Samples were prepared using dry and degassed deuterated solvents, under inert atmosphere. The samples were run on Jeol ECP(Eclipse) 300 MHz and Jeol ECS 400 MHz multinuclear spectrometers and Varian 400-MR and VNMR500 instruments. Variable temperature experiments were carried out solely on the Jeol ECS 300 MHz multinuclear spectrometer. ¹H and ¹³C spectra were referenced to internal solvent peaks, ³¹P NMR spectra were referenced to an external sample of 85% H₃PO₄ and ⁷⁷Se NMR spectra were referenced to an external sample of Na₂SeO₃.

Elemental analysis (C, H and N) was obtained using a Carlo Erba EA1108 CHN elemental analyser at the University of Bristol. Air and moisture sensitive samples were loaded into aluminium boats in a glove box atmosphere.

Single Crystal X-ray Crystallography

Crystals were removed directly from the mother liquor under nitrogen and protected from air, moisture and solvent loss using sodium dried heavy paraffin oil. Crystals were selected using an optical microscope and mounted on a glass fibre attached to a brass pin which was quickly transferred to the cold nitrogen stream of the diffractometer. Measurements were collected on a Bruker-AXS SMART APEX II three circle diffractometer employing Mo-K_α radiation (λ = 0.71073 Å). Intensities were integrated from several series of exposures, each exposure covering 0.3° in ω. Absorption corrections were applied based on multiple and symmetry-equivalent measurements. The structures were solved by direct methods and refined by least squares on weighted F² values for all reflections. All non-hydrogen atoms were assigned anisotropic displacement parameters and refined without positional constraints. Hydrogen atoms were constrained to ideal geometries and refined with fixed isotropic displacement parameters.

Synthesis of 1, 2

PhECl (E = S or Se; 1 mmol) was added to a clear solution of GaCl₃ (1 mmol, 176 mg) in CH₂Cl₂ (10 mL) and stirred for 5 mins resulting in a dark orange solution. PPh₃ (1 mmol, 262 mg) was added and the resulting colourless solution was stirred

for 1 h. The solution was concentrated and recrystallized from a saturated CH₂Cl₂ solution layered with *n*-hexane.

Data for 1: 536 mg (85%), ¹H NMR (400 MHz, 20 °C, CD₂Cl₂) δ_H 7.93-7.90 (m, 2H, H⁵), 7.68-7.63 (m, 1H, H⁶), 7.58-7.54 (m, 2H, H⁴), 1.70 (d, ³J_{H-P} = 15.0 Hz, 27H, H²) ppm.

¹³C{¹H} NMR (100 MHz, 20 °C, CD₂Cl₂) δ_C 138.47 (d, ³J_{C-P} = 2.9 Hz, C⁴), 133.03 (d, ³J_{C-P} = 2.4 Hz, C⁶), 131.29 (d, ⁴J_{C-P} = 2.3 Hz, C⁵), 46.45 (d, ¹J_{C-P} = 15.4 Hz, C¹), 30.98 (s, C²) ppm (no peak observed for C³).

³¹P{¹H} NMR (121 MHz, 20 °C, CD₂Cl₂) δ_P 85.7 ppm.

Calc. for C₂₄H₂₀Cl₄GaPS: C, 49.40; H, 3.43; Found: C, 49.85; H, 3.47 %

Single crystal X-ray diffraction data: C₂₄H₂₀Cl₄GaPS, *M* = 582.95, Monoclinic, *a* = 9.6073(2), *b* = 13.5295(3), *c* = 10.0002(2), α = 90, β = 102.2060(10), γ = 90, *V* = 1270.46(5), *T* = 100(2) K, space group *P*2₁, *Z* = 2, μ(MoKα) = 1.524 mm⁻¹, 43043 reflections measured, 5844 independent reflections (*R*_{int} = 0.0236). The final *R*₁ [*I* > 2σ(*I*)] was 0.0161 and the final *wR*(*F*₂) was 0.0400 [*I* > 2σ(*I*)]. The goodness of fit on *F*² was 1.057. CCDC 1015637.

Data for 2: 454 mg (78%), ¹H NMR (400 MHz, 20 °C, CD₂Cl₂) δ_H 7.93-7.88 (3H, m, 3 × H⁴), 7.75-7.69 (6H, m, 6 × H³), 7.63-7.52 (7H, m, 6 × H², 1 × H⁸), 7.35-7.27 (4H, m, 2 × H⁶, 2 × H⁷) ppm.

¹³C{¹H} NMR (100 MHz, 20 °C, CD₂Cl₂) δ_C 138.35 (s, C⁶), 136.56 (d, ⁴J_{C-P} = 3.1 Hz, C⁴), 134.46 (d, ³J_{C-P} = 10.9 Hz, C²), 132.61 (s, C⁸), 131.42 (s, C⁷), 131.14 (d, ³J_{C-P} = 13.9 Hz, C³), 119.51 (s, C⁵), 118.85 (d, ¹J_{C-P} = 77.8 Hz, C¹) ppm.

³¹P{¹H} NMR (121.4 MHz, 20 °C, CH₂Cl₂) δ_P 38.3 ppm (s, satellites from ¹J_{P-Se} = 455.90 Hz).

⁷⁷Se NMR (53.4 MHz, 20 °C, CD₂Cl₂) δ_{Se} 300 (d, ¹J_{Se-P} = 455.90 Hz) ppm.

Calc. for C₂₄H₂₀Cl₄GaPSe: C, 45.76; H, 3.20; Found: C, 46.13; H, 3.23 %

Single crystal X-ray diffraction data: C₂₄H₂₀Cl₄GaPSe, *M* = 629.85, Monoclinic, *a* = 9.6355(4), *b* = 13.5694(5), *c* = 10.0151(4), α = 90, β = 102.248(2), γ = 90, *V* = 1279.65(9), *T* = 100(2) K, space group *P*2₁, *Z* = 4, μ(MoKα) = 2.998 mm⁻¹, 8294 reflections measured. The final *R*₁ [*I* > 2σ(*I*)] was 0.0365 and the final *wR*(*F*₂) was 0.0761 [*I* > 2σ(*I*)]. The goodness of fit on *F*² was 1.038. The crystal was twinned and data was merged so no *R*_{int} value is calculated. CCDC 1015640.

Synthesis of 3, 4

[PhEPPPh₃][SbF₆] {**1** (E = S) or **2** (E = Se); 1 mmol) was prepared *in situ* as described above. One equivalent of tri-*tert*-butylphosphine (1 mmol, 202 mg) was added and the solution was stirred for 2 h. The solution was concentrated and recrystallized from a saturated CH₂Cl₂ solution layered with *n*-hexane.

Data for 3: 396 mg (72%), ¹H NMR (400 MHz, 20 °C, CD₂Cl₂) δ_H 7.93-7.90 (m, 2H, H⁵), 7.68-7.63 (m, 1H, H⁶), 7.58-7.54 (m, 2H, H⁴), 1.70 (d, ³J_{H-P} = 15.0 Hz, 27H, H²) ppm.

¹³C{¹H} NMR (100 MHz, 20 °C, CD₂Cl₂) δ_C 138.47 (d, ³J_{C-P} = 2.9 Hz, C⁴), 133.03 (d, ⁵J_{C-P} = 2.4 Hz, C⁶), 131.29 (d, ⁴J_{C-P} = 2.3 Hz, C⁵), 46.45 (d, ¹J_{C-P} = 15.4 Hz, C¹), 30.98 (s, C²) ppm (no peak observed for C³).

³¹P{¹H} NMR (121 MHz, 20 °C, CD₂Cl₂) δ_P 85.7 ppm.

Calc. for C₁₈H₃₂F₆PSSbS: C, 39.51; H, 5.89; Found: C, 40.11; H, 5.92 %

Single crystal X-ray diffraction data: C₁₈H₃₂F₆PSSb, *M* = 547.22, Orthorhombic, *a* = 8.2990(6), *b* = 17.4242(13), *c* = 15.3754(15), α = 90, β = 90, γ = 90, *V* = 2223.5(3), *T* = 100(2) K, space group *Pbcm*, *Z* = 4, μ(MoKα) = 1.457 mm⁻¹, 13811

reflections measured, 3205 independent reflections ($R_{int} = 0.0896$). The final R_1 [$I > 2\sigma(I)$] was 0.1274 and the final $wR(F_2)$ was 0.2614 [$I > 2\sigma(I)$]. The goodness of fit on F^2 was 1.206. The crystal was twinned and data was merged so no R_{int} value is calculated.

Data for 4: 523 mg (88%), $^1\text{H NMR}$ (400 MHz, 20 °C, CD_2Cl_2) δ_{H} 7.96-7.92 (m, 2H, H^5), 7.63-7.58 (m, 1H, H^6), 7.52-7.47 (m, 2H, H^4), 1.69 (d, $^3J_{\text{H-P}} = 16.0$ Hz, 27H, H^2) ppm.

$^{13}\text{C}\{^1\text{H}\}$ NMR (125 MHz, 20 °C, CD_2Cl_2) δ_{C} 139.34 (d, $^3J_{\text{C-P}} = 2.3$ Hz, C^4), 132.61 (d, $^5J_{\text{C-P}} = 2.3$ Hz, C^6), 131.23 (d, $^4J_{\text{C-P}} = 2.2$ Hz, C^5), 120.11 (d, $^2J_{\text{C-P}} = 9.6$ Hz, C^3), 46.16 (d, $^1J_{\text{C-P}} = 11.4$ Hz, C^1), 30.93 (s, C^2) ppm.

$^{31}\text{P}\{^1\text{H}\}$ NMR (200 MHz, 20 °C, CD_2Cl_2) δ_{P} 89.0 (satellites from $^1J_{\text{P-Se}} = 481.3$ Hz) ppm.

Calc. for $\text{C}_{18}\text{H}_{32}\text{F}_6\text{PSbSe}$: C, 36.39; H, 5.43; Found: C, 36.92; H, 5.43 %

Single crystal X-ray diffraction data: $\text{C}_{36}\text{H}_{64}\text{F}_{12}\text{P}_2\text{Sb}_2\text{Se}_2$, $M = 1188.23$, Monoclinic, $a = 8.4039(3)$, $b = 15.0539(5)$, $c = 35.2907(11)$, $\alpha = 90$, $\beta = 90.01$, $\gamma = 90$, $V = 4464.7(3)$, $T = 100(2)$ K, space group $P2_1/c$, $Z = 4$, $\mu(\text{MoK}\alpha) = 2.988$ mm^{-1} , 59130 reflections measured, 10231 independent reflections ($R_{int} = 0.0284$). The final R_1 [$I > 2\sigma(I)$] was 0.0231 and the final $wR(F_2)$ was 0.0615 [$I > 2\sigma(I)$]. The goodness of fit on F^2 was 1.219.

Synthesis of 5, 6

(MeE) $_2$ (E = S or Se; 0.1 mmol) was added to a suspension of AgSbF_6 (0.1 mmol, 34 mg) in CD_2Cl_2 (1 mL) and shaken until solid precipitates. The solids were removed by syringe filtration and the filtrate was added to an NMR tube charged with PPh_3 (0.1 mmol, 26 mg). Characterisation data was limited to the following analytical data which were obtained on these crude solutions.

Data for 5: $^1\text{H NMR}$ (500 MHz, 21 °C, CD_2Cl_2) δ_{H} 7.98-7.92 (m, 3H, H^4), 7.83-7.76 (m, 12H, $3 \times \text{H}^3$, $3 \times \text{H}^2$), 2.43 (d, $^3J_{\text{H-P}} = 15.0$ Hz, 3H, H^5) ppm.

$^{13}\text{C}\{^1\text{H}\}$ NMR (125.7 MHz, 21 °C, CD_2Cl_2) δ_{C} 136.2 (d, $^4J_{\text{C-P}} = 3.4$ Hz, C^4), 133.5 (d, $^2J_{\text{C-P}} = 10.9$ Hz, C^2), 130.8 (d, $^3J_{\text{C-P}} = 13.6$ Hz, C^3), 117.9 (d, $^1J_{\text{C-P}} = 85.3$ Hz, C^1), 13.4 (d, $^2J_{\text{C-P}} = 4.3$ Hz, C^5) ppm.

$^{31}\text{P}\{^1\text{H}\}$ NMR (160 MHz, 21 °C, CD_2Cl_2) δ_{P} 46.5 ppm.

Data for 6: $^1\text{H NMR}$ (500 MHz, 21 °C, CD_2Cl_2) δ_{H} 7.95-7.90 (m, 3H, H^4), 7.82-7.73 (m, 12H, $6 \times \text{H}^3$, $6 \times \text{H}^2$), 2.35 (d, $^3J_{\text{H-P}} = 13.14$ Hz, 3H, H^5) ppm.

$^{13}\text{C}\{^1\text{H}\}$ NMR (125 MHz, 21 °C, CD_2Cl_2) δ_{C} 136.0 (d, $^4J_{\text{C-P}} = 3.4$ Hz, C^4), 133.5 (d, $^2J_{\text{C-P}} = 11.0$ Hz, C^2), 130.8 (d, $^3J_{\text{C-P}} = 13.6$ Hz, C^3), 118.5 (d, $^1J_{\text{C-P}} = 78.6$ Hz, C^1), 8.2 (d, $^2J_{\text{C-P}} = 3.1$ Hz, C^5) ppm.

$^{31}\text{P}\{^1\text{H}\}$ NMR (200 MHz, 21 °C, CD_2Cl_2) δ_{P} 36.7 (satellites from $^1J_{\text{P-Se}} = 451.6$ Hz) ppm.

Conclusions

In summary, we have prepared a range of thio- and seleno-phosphonium cationic complexes $[\text{RE}(\text{PR}'_3)]^+[\text{X}]^-$ (R = Me, Ph; E = S, Se; X = GaCl_4 , SbF_6) and presented experimental evidence showing degenerate exchange reaction of the phosphine ligand between these cationic complexes and free phosphine occurs via an associative ($\text{S}_{\text{N}}2$ type) reaction. The rate of exchange increases when comparing sulfur to selenium. Furthermore, for species with R = aryl substituents, exchange was observed to be faster than those with R = alkyl

substituents. These conclusions are supported by DFT calculations.

Acknowledgements

We thank the University of Bristol for funding (L.C.F).

Notes and references

^a School of Chemistry, University of Bristol, Bristol, BS8 1TS

Chris.Russell@bristol.ac.uk;

<http://www.inchm.bris.ac.uk/people/russell/Index2.htm>

^b Department of Chemistry, University of York, Heslington, York, YO10

SDD E-mail: John.Slattery@york.ac.uk

† The naming of these species suffers the same quandary as the corresponding $[\text{R}_2\text{P}-\text{PR}'_3]^+$ cations which are named either as phosphonium-phosphine cations or phosphine-phosphonium cations, depending on the atom to which the positive charge is formally assigned. In this study, we have chosen to use the name based on chalcogen phosphonium salts for the cations $[\text{REPR}'_3]^+$, although we do not seek to imply that this is necessarily a reflection on the assignment of formal charge.

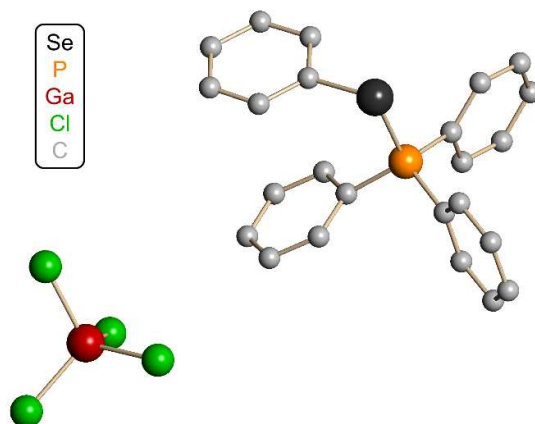
‡ Care should be taken with calculated free energy changes, as entropy changes in solution are known to be overestimated by gas-phase calculations.²¹

Electronic Supplementary Information (ESI) available: Details of all computational studies can be found in the ESI. See DOI: 10.1039/b000000x/

1. a) J. C. Sheehan and K. R. Henery-Logan, *J. Am. Chem. Soc.*, 1957, **79**, 1262-1263; b) R. D. G. Cooper, L. D. Hatfield and D. O. Spry, *Acc. Chem. Res.*, 1973, **6**, 32-40; c) S. J. Dancer, *J. Antimicrob. Chemother.*, 2001, **48**, 463-478.
2. a) C. M. Weekley and H. H. Harris, *Chem. Soc. Rev.*, 2013, **42**, 8870-8894; b) R. Bentley, *Chem. Soc. Rev.*, 2005, **34**, 609-624.
3. H. Pellissier, *Chiral Sulfur Ligands Asymmetric Catalysis*, Royal Society of Chemistry, Cambridge, UK, 2009.
4. a) C. Paulmier, *Selenium Reagents and Intermediates in Organic Synthesis*, Pergamon Press, 1986; b) E. Block, *Reactions of Organosulfur Compounds*, Academic Press Inc. Ltd., London, 1978; c) T. Wirth, *Tetrahedron*, 1999, **55**, 1-28; d) A. J. Mukherjee, S. S. Zade, H. B. Singh and R. B. Sunoj, *Chem. Rev.*, 2010, **110**, 4357-4416; e) T. G. Back, *Organoselenium Chemistry A Practical Approach*, Oxford University Press, New York, 1999.
5. a) J. Beckmann, J. Bolsinger, A. Duthie, P. Finke, E. Lork, C. Lütke, O. Mallow and S. Mebs, *Inorg. Chem.*, 2012, **51**, 12395-12406; b) J. W. Dube, M. M. Hänninen, J. L. Dutton, H. M. Tuononen and P. J. Ragogna, *Inorg. Chem.*, 2012, **51**, 8897-8903; c) K. Sugamata, T. Sasamori and N. Tokitoh, *Eur. J. Inorg. Chem.*, 2012, **2012**, 775-778; d) S. S. Zade and H. B. Singh, in *PATAI'S Chemistry of Functional Groups*, John Wiley & Sons, Ltd, 2009.
6. a) T. Wirth, G. Fragale and M. Spichty, *J. Am. Chem. Soc.*, 1998, **120**, 3376-3381; b) S. E. Denmark, W. R. Collins and M. D. Cullen, *J. Am. Chem. Soc.*, 2009, **131**, 3490-3492.
7. X. Wang, K. N. Houk, M. Spichty and T. Wirth, *J. Am. Chem. Soc.*, 1999, **121**, 8567-8576.
8. T. I. Sølling, S. B. Wild and L. Radom, *Chem. Eur. J.*, 1999, **5**, 509-514.
9. T. I. Sølling, M. A. McDonald, S. B. Wild and L. Radom, *J. Am. Chem. Soc.*, 1998, **120**, 7063-7068.
10. a) G. I. Borodkin, E. I. Chernyak, M. M. Shakirov and V. G. Shubin, *Russ. J. Org. Chem.*, 1997, **33**, 418-419; b) G. I. Borodkin, E. I. Chernyak, M. M. Shakirov and V. G. Shubin, *Russ. J. Org. Chem.*, 1998, **34**, 1563-1568.

Journal Name

11. S. E. Denmark, D. Kalyani and W. R. Collins, *J. Am. Chem. Soc.*, 2010, **132**, 15752-15765.
12. J. M. Slattery, C. Fish, M. Green, T. N. Hooper, J. C. Jeffery, R. J. Kilby, J. M. Lynam, J. E. McGrady, D. A. Pantazis, C. A. Russell and C. E. Willans, *Chem. Eur. J.*, 2007, **13**, 6967-6974.
13. N. S. Townsend, S. R. Shadbolt, M. Green and C. A. Russell, *Angew. Chem. Int. Ed.*, 2013, **52**, 3481-3484.
14. N. A. Barnes, S. M. Godfrey, R. T. A. Halton, I. Mushtaq, R. G. Pritchard and S. Sarwar, *Dalton Trans.*, 2006, 1517-1523.
15. S. Kubiniok, W.-W. du Mont, S. Pohl and W. Saak, *Angew. Chem. Int. Ed.*, 1988, **27**, 431-433.
16. P. D. Boyle, S. M. Godfrey, C. A. McAuliffe, R. G. Pritchard and J. M. Sheffield, *Chem. Commun.*, 1999, 2159-2160.
17. N. A. Barnes, S. M. Godfrey, R. T. A. Halton, I. Mushtaq and R. G. Pritchard, *Dalton Trans.*, 2006, 4795-4804.
18. P. G. Jones and C. Thöne, *Z. Kristallogr. - Cryst. Mat.*, 1994, **209**, 78-79.
19. a) G. I. Borodkin, E. I. Chernyak, M. M. Shakirov and V. G. Shubin, *Russ. J. Org. Chem.*, 1997, **33**, 418-419; b) G. I. Borodkin, E. I. Chernyak, M. M. Shakirov and V. G. Shubin, *Russ. J. Org. Chem.*, 1998, **34**, 1563-1568.
20. M. B. Hursthouse, K. M. A. Malik, D. E. Hibbs, S. M. Roberts, A. J. H. Seago, V. Sik and R. Storer, *Journal of the Chemical Society-Perkin Transactions 1*, 1995, 2419-2425.
21. a) B. O. Leung, D. L. Reid, D. A. Armstrong and A. Rauk, *The Journal of Physical Chemistry A*, 2004, **108**, 2720-2725; b) D. Ardura, R. López and T. L. Sordo, *The Journal of Physical Chemistry B*, 2005, **109**, 23618-23623; c) P. A. Dub and R. Poli, *J. Mol. Catal. A: Chem.*, 2010, **324**, 89-96.

Table of Contents Entry

The phosphine unit of cationic thio- and seleno-phosphonium complexes exchange via a $\text{S}_{\text{N}}2$ -type exchange process.